On the Contact Duration Accuracy of Discrete-Time Collision Models

Vasileios Chatziioannou,[1†] *Maarten van Walstijn,*[2]

[1]Department of Music Acoustics, University of Music and Performing Arts Vienna, Austria
[2]Sonic Arts Research Centre, Queen's University Belfast, UK
[†]chatziioannou@mdw.ac.at

ABSTRACT

Collisions are a vital part of the function of musical instruments. They occur in various forms and during different phases of oscillation, including transient and steady-state regimes. The non-smooth nature of the nonlinearity inherent to objects coming into contact and decoupling again poses several difficulties when it comes to formulating numerical models. Besides issues regarding numerical stability – that have recently been handled using energy methods – questions arise about how accurately different numerical schemes can approximate the trajectories of colliding objects. This paper presents a comparative analysis of two particular types of time-stepping algorithms (namely a two-point, two-variable and a three-point, one-variable scheme) employed to simulate contact between a mass and a barrier. Focusing largely on cases for which the exact solution is known, the schemes are evaluated in terms of their ability to simulate the correct duration of contact.

1. INTRODUCTION

Many musical instruments feature mechanical collisions that can be assumed elastic or semi-elastic, with the contact characteristics determined mostly by the impact velocity and the material and geometrical properties of the colliding objects. Such collisions can be modelled by defining a repelling force that is non-zero only for negative inter-object distance, which corresponds to object compression. In music acoustics, this contact force is often defined in power law form, the parameters of which determine the duration and level of the compression. Having a physical basis in Hertzian contact theory, it provides simple and effective control over the collision characteristics, ranging from soft (e.g. hammer-string interaction [1]) to hard collisions (e.g. string-bridge contact [2]).

Incorporation of power-law contact into time-stepping schemes requires to observe the energy balance of the underlying continuous-domain system, as otherwise numerical stability issues may arise. Several methods for deriving energy-stable schemes have been proposed recently, with the discretisation performed over either a first-order [3, 4, 5] or a second-order [6, 7, 8] form. A recent study on modelling distributed string-barrier contact [9] has reported indications that the latter type is more prone to spurious oscillations. The present study makes further inroads into the understanding of the accuracy of these schemes by investigating impactive contact between a single mass and a barrier, focusing on errors in the contact duration.
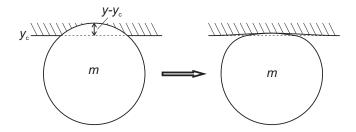

Figure 1. Left: mass-wall collision where the penetration argument $y - y_\mathrm{c}$ is defined; Right: the equivalent physical setting, showing the compression of the mass and the wall.

2. MASS-WALL COLLISION

Consider a (lumped) mass approaching a wall from below. The collision force can be modelled using a one-sided power law [10]. This may be formulated as

$$f(y) = -k_\mathrm{c}\lfloor(y - y_\mathrm{c})\rfloor^{\alpha}, \qquad (1)$$

where y is the mass displacement, k_c the collision stiffness, α a power-law constant, y_c the location of the wall and $\lfloor\chi\rfloor^{\alpha} = h(\chi)\chi^{\alpha}$, $h(\chi)$ being the Heaviside step function. Hence $y - y_\mathrm{c}$ corresponds to the compression of the colliding objects (see Figure 1, noting that both the moving mass and the wall are assumed to get compressed during collision). The net amount of compression is controlled in the model by the contact parameters k_c and α. For simplicity, in what follows y_c is set equal to zero. Defining the collision force potential as

$$V(y) = \frac{k_\mathrm{c}}{\alpha + 1}\lfloor y \rfloor^{\alpha+1} := \frac{k_\mathrm{c}}{\alpha + 1}G(y) \qquad (2)$$

the equation of motion for the mass m reads

$$m\frac{\mathrm{d}^2 y}{\mathrm{d}t^2} = -\frac{\partial V}{\partial y} \qquad (3)$$

hence the Hamiltonian (total energy) of the system is

$$H(y,p) = \frac{p^2}{2m} + \frac{k_\mathrm{c}}{\alpha + 1}\lfloor y \rfloor^{\alpha+1}, \qquad (4)$$

where p is the conjugate momentum, with

$$\frac{\mathrm{d}H}{\mathrm{d}t} = \frac{\partial H}{\partial y}\frac{\mathrm{d}y}{\mathrm{d}t} + \frac{\partial H}{\partial p}\frac{\mathrm{d}p}{\mathrm{d}t} = k_\mathrm{c}\lfloor y \rfloor^{\alpha}\frac{p}{m} + \frac{p}{m}m\frac{\mathrm{d}^2 y}{\mathrm{d}t^2} \overset{(3)}{=} 0 \qquad (5)$$

so, in the absence of damping terms, the energy of the system remains constant.

three-point
one-variable $\circ$- - - $\bullet$- - - $\bullet$- - - $\bullet$- - - $\circ$
y^{n-2} y^{n-1} y^n y^{n+1} y^{n+2}

two-point
two-variable $\circ$- - - $\circ$- - - $\bullet$- - - $\bullet$- - - $\circ$
y^{n-2} y^{n-1} y^n y^{n+1} y^{n+2}
q^{n-2} q^{n-1} q^n q^{n+1} q^{n+2}

Figure 2. Three-point (top) and two-point (bottom) temporal stencils.

2.1. Discretisation

Two different starting points may be used for the discretisation of the above problem. Either Newton's equation of motion (3) can be directly discretised, or the problem can be first written using Hamilton's equations [11]. The former approach requires the numerical solution of a single, second-order differential equation, whereas the latter is based on the solution of two first-order equations, namely

$$\frac{\mathrm{d}y}{\mathrm{d}t} = \frac{\partial H(y,p)}{\partial p} = \frac{p}{m}, \tag{6a}$$

$$\frac{\mathrm{d}p}{\mathrm{d}t} = -\frac{\partial H(y,p)}{\partial y} = -\frac{\partial V(y)}{\partial y}. \tag{6b}$$

Note that this first order form can be also obtained from the Newtonian description, by reducing the single second-order differential equation (3) to two first-order ones (see, e.g. [12]).

Discretising Newton's equation of motion (as in [6]) yields the following numerical scheme

$$y^{n+1} - 2y^n + y^{n-1} = -\beta_3 \frac{G(y^{n+1}) - G(y^{n-1})}{y^{n+1} - y^{n-1}}, \tag{7}$$

where $\beta_3 = (k_c \Delta t^2)/(m(\alpha+1))$ and y^n denotes the value of variable y at time $n\Delta t$, with $\Delta t = 1/f_s$ (f_s being the sampling rate). Equation (7) can be said to form a three-point, one-variable scheme, since its temporal stencil encompasses three grid points (see Figure 2 top). On the other hand, discretising Hamilton's equations using mid-point derivative approximations and setting $q^n = p^n \Delta t/(2m)$ (see [4]) yields

$$y^{n+1} - y^n = q^{n+1} + q^n \tag{8a}$$

$$q^{n+1} - q^n = -\beta_2 \frac{G(y^{n+1}) - G(y^n)}{y^{n+1} - y^n}, \tag{8b}$$

which is a two-point, two-variable scheme[1] (see Figure 2 bottom) with $\beta_2 = \beta_3/2$. Both schemes (7) and (8) are written in terms of two parameters, namely α and $\beta_\kappa, \kappa = 2, 3$, and can be shown to be second order accurate[2] for $\alpha > 1$, as well as numerically stable for $\beta_\kappa \geq 0$ (see [4, 10]) which holds unconditionally. The equations are nonlinear due to the presence of the collision term and may be solved using an iterative
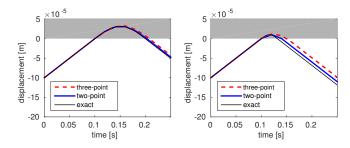
---

[1]Note that, as explained in [4], under linear conditions this scheme is equivalent to both the trapezoidal rule and the implicit mid-point rule. However, in the presence of nonlinear forces, such as those acting during collisions, all three schemes are distinct (and only (8) is energy conserving).

[2]for $\alpha = 1$ only first order accuracy can be inferred, since $G(y)$ is not twice differentiable at $y = 0$.

Figure 3. Mass displacement for a 'soft' (left) and a 'hard' collision (right). The red dashed curve corresponds to the three-point scheme and the blue curve to the two-point scheme, whereas the black line represents the exact solution.

method (such as Newton's method). Figure 3 shows simulations of a softer ($\alpha = 1$, $k_c = 10^9$) and a harder collision ($\alpha = 1$, $k_c = 10^{10}$) of a 1 kg mass approaching a barrier from below with initial displacement $y(0) = -0.1$ mm and velocity $v(0) = 1$ m/s. The sampling rate is $f_s = 50$ kHz.

In both plots, a difference in the contact duration τ_c is observed. This appears to be a systematic phenomenon that is particularly significant for hard impacts. One way to get insight into what causes these differences is to consider, for each scheme, whether it is possible to 'exit' the wall immediately after entering it. For the three-point scheme, this amounts to investigating the mapping in equation (7). Exiting the wall one time step after entering implies $\{ y^{n-1} \leq 0, \ y^n > 0 \} \Rightarrow y^{n+1} \leq 0$. Defining $y^{n-1} = -\delta$ and $y^n = \epsilon$, with $\delta \geq 0, \epsilon > 0$, equation (7) can then be written as

$$y^{n+1} = 2\epsilon + \delta - \beta_3 \frac{G(y^{n+1}) - G(-\delta)}{y^{n+1} + \delta}. \tag{9}$$

Considering the form of the collision potential and requiring y^{n+1} to be nonpositive yields $y^{n+1} = 2\epsilon + \delta > 0$ which is a contradiction. Hence, under the three-point scheme the mass-wall interaction can never be confined to a single time-step. On the other hand, if both $y^{n-1}, y^n > 0$ then the resulting equation (assuming $y^{n+1} \leq 0$ and setting $y^{n-1} = \eta > 0$) reads

$$y^{n+1} = 2\epsilon - \eta - \beta_3 \frac{G(\eta)}{\eta - y^{n+1}}, \tag{10}$$

which is of indeterminate sign. Hence, after having remained within the barrier for two time steps, the mass has the possibility to exit at the next time step. Hence, the minimum contact duration that this scheme can simulate is equal to $2\Delta t$, (i.e. $\tau_c \geq 2\Delta t$).

For the two-point scheme a similar calculation can be performed to show that $\tau_c \geq \Delta t$. The numerical scheme (8) may be written as

$$y^{n+1} = y^n + 2q^n - \beta_2 \frac{G(y^{n+1}) - G(y^n)}{y^{n+1} - y^n}. \tag{11}$$

The condition for a collision to occur is that, in the absence of a contact force, the mass will 'enter' the barrier at the next time step, which is equivalent to
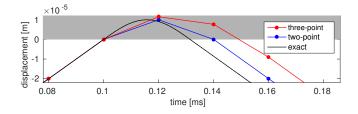
Figure 4. Detail of the mass displacement across the barrier in the case of a hard collision. Notice that only the two-point scheme simulates an impact force of a single time step.

$\{\, y^n \leq 0, \ q^n > 0 \,\} \Rightarrow \hat{y}^{n+1} > 0$, where $\hat{y}^{n+1}$ is the virtual displacement at the next time step had the collision force not been present (i.e. for $\beta_2 = 0$). Defining $y^n = -\zeta$ and $q^n = \mu$, with $\zeta \geq 0, \mu > 0$ leads to

$$\hat{y}^{n+1} = 2\mu - \zeta > 0. \quad (12)$$

We proceed to show that in the presence of a contact force the mass will spend at least one time instant within the barrier (i.e. $y^{n+1} > 0$). Assume that this is false and $y^{n+1} \leq 0$. Then

$$y^{n+1} = 2\mu - \zeta - \beta_2 \frac{G(y^{n+1}) - G(-\zeta)}{y^{n+1} + \zeta} = 2\mu - \zeta \overset{(12)}{>} 0, \quad (13)$$

which is a contradiction. Hence $y^{n+1} > 0$ and $\tau_c \geq \Delta t$.

Furthermore, it can be shown that after having spent one time instant within the barrier, the mass has the possibility to exit the barrier (with the following displacement value being of indeterminate sign). So any contact duration higher than Δt may be simulated by the two-point scheme. This is visualised in Figure 4, which shows the details of a contact with ($\alpha = 1$, $k_c = 10^{11}$), the remaining parameters being as in Figure 3. The fact that the two-point scheme may simulate shorter contact durations results in a smaller error compared to the three-point scheme. This error comparison is further discussed in the next section where the possibility of simulating the correct contact duration is explored.

3. EXACT SOLUTION FOR $\alpha = 1$

For $\alpha = 1$, and initial conditions $y(0) = -d$, $v(0) = v_0$, an exact solution can be obtained in the form of a continuous, twice differentiable piecewise function

$$y(t) = \begin{cases} -d + v_0 t & : \quad 0 \leq t < t_1 \\ \dfrac{v_0}{\omega_c} \sin\big(\omega_c(t - t_1)\big) & : \quad t_1 \leq t < t_2 \\ -v_0(t - t_2) & : \quad t \geq t_2 \end{cases}, \quad (14)$$

where $t_1 = d/v_0$ and $t_2 = t_1 + \tau_c$ are the time of impact and release, respectively, and where $\omega_c = \sqrt{k_c/m}$ is the natural frequency that would occur if the potential in (2) was always 'active', i.e. if $V(y) = \frac{1}{2}k_c y^2$. The contact duration is $\tau_c = \pi/\omega_c$, which corresponds to a half cycle of a sinusoidal waveform of frequency ω_c.

Both schemes presented in the previous section can – within certain limits – be made exact in terms of this contact duration (i.e. having the correct natural frequency ω_c). For the

two-point scheme this is achieved via the substitution

$$\beta_2 \to \beta_2^* = \frac{1 - \cos(\omega_c \Delta t)}{1 + \cos(\omega_c \Delta t)}, \quad (15)$$

with the constraint that $\omega_c < \pi/\Delta t$, as otherwise the natural frequency exceeds the Nyquist frequency (i.e. is aliased). This substitution, that can be derived using frequency-domain analysis (see, e.g. Sec. 2.3 in [5]), ensures that the numerical scheme has the correct contact duration. Note that numerical stability is not affected, because the condition $\beta_2^* \geq 0$ is still satisfied unconditionally. The non-aliasing constraint translates to a lower bound $\tau_c > \Delta t$ on the contact duration.

For the three-point scheme the equivalent substitution to obtain the correct contact duration (again for $\alpha = 1$) is

$$\beta_3 \to \beta_3^* = \frac{1 - \cos(\omega_c \Delta t)}{\cos(\omega_c \Delta t)}. \quad (16)$$

However another, more severe constraint $\omega_c < \frac{1}{2}\pi/\Delta t$ applies now, because otherwise β_3^* is not guaranteed to be non-negative. This stability constraint translates to a lower bound $\tau_c > 2\Delta t$ on the contact duration. Hence both schemes can be made exact in terms of their oscillatory behaviour (see Figure 5) up to a minimum contact duration (for a given sampling rate) which is twice as small for the two-point scheme, in comparison to the three-point scheme. When it is required to simulate contacts with durations shorter than this lower bound this substitutions can only be performed to the limit that aliasing is avoided and β_κ remains non-negative. Hence an error is introduced which can be quantified as the difference between the exact and the simulated contact duration.

Note that these lower bounds on τ_c are in agreement with those calculated in the previous section from the discrete update equations, for arbitrary values of α. Figure 6 shows (for the parameters of the hard collision in the previous section) the minimum contact duration that may be exactly simulated using each scheme, as a function of the sampling rate. The bottom plot shows the error that is introduced by each approximation when shorter durations need to be simulated.

From the above analysis it can be extracted that (1) the two-point scheme can exactly simulate contacts of durations twice as short as the three-point scheme and (2) when even shorter contact durations need to be simulated the error introduced by the three-point scheme is significantly larger.
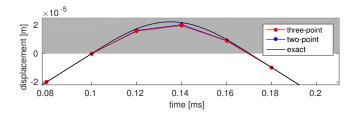

Figure 5. Detail of the mass displacement across the barrier when the corrected values β_2^* and β_3^* are used for $\omega_c = 44700$ rad/s.
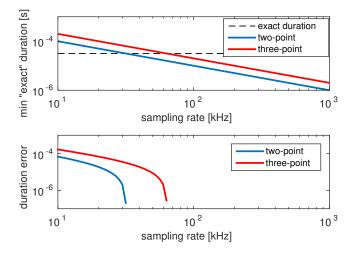
Figure 6. Top: the minimum contact duration that each scheme can simulate exactly for different sampling rates (for the parameters of the hard collision of Figure 3). The dashed line indicates an example target duration. Bottom: the error introduced in the contact duration when it is too short to be simulated exactly for a given sampling rate.

4. CONCLUSIONS

In this paper two different schemes (that have recently seen much application in simulation of musical instrument contact dynamics) have been analysed, based on their ability to simulate the colliding mass trajectory. In particular, it has been shown that different results are obtained, especially for hard collision cases, where the reference contact duration is of the order of the sampling interval.

In the context of music acoustics research, the ability of a numerical scheme to accurately model the contact duration time can be important. Note onsets are often related to impactive excitations, so simulations of transients may be affected by inaccuracies in the underlying collision model. Furthermore, when repeated impacts are simulated (as is the case for example in instruments involving string-barrier collisions, such as a sitar or a snare drum) the periodicity and/or spectral evolution are affected by the contact duration (see, for example, [13]). So in general, the time step has to be chosen sufficiently small to enable to compute the results for a particular study without significant error. As such it is advantageous if the required accuracy can be achieved with a lower sample rate, which is what the two-point scheme offers over the three-point scheme.

An interesting future research direction would be to investigate whether and how model parameters could be set to better approximate contact durations for cases when $\alpha > 1$. Another question that arises from this study is to what extent the differences between two-point, two-variable and three-point, one-variable schemes are potentially significant for other types of musical instrument nonlinearity and/or for time-variant components of musical instruments.

5. ACKNOWLEDGEMENTS

REFERENCES

[1] A. Chaigne and J. Kergomard, *Acoustics of Musical Instruments*. New York: Springer, 2016.

[2] M. van Walstijn and V. Chatziioannou, "Numerical simulation of tanpura string vibrations," in *Proc. Int. Symp. Musical Acoustics*, Le Mans, 2014, pp. 609–614.

[3] V. Chatziioannou and M. van Walstijn, "An energy conserving finite difference scheme for simulation of collisions," in *Proc. Sound and Music Computing (SMAC-SMC 2013)*, Stockholm, 2013, pp. 584–591.

[4] V. Chatziioannou and M. van Walstijn, "Energy conserving schemes for the simulation of musical instrument contact dynamics," *Journal of Sound and Vibration*, vol. 339, pp. 262–279, 2015.

[5] M. van Walstijn, J. Bridges, and S. Mehes, "A real-time synthesis oriented tanpura model," in *Proc. Int. Conf. Digital Audio Effects (DAFx-16)*, 2016.

[6] S. Bilbao, A. Torin, and V. Chatziioannou, "Numerical modeling of collisions in musical instruments," *Acta Acustica united with Acustica*, vol. 101, no. 1, pp. 155–173, 2015.

[7] M. Ducceschi, S. Bilbao, and C. Desvages, "Modelling collisions of nonlinear strings against rigid barriers: Conservative finite difference schemes with application to sound synthesis," in *Proc. 22nd Int. Congress on Acoustics*, Buenos Aires, 2016.

[8] J. Chabassier, A. Chaigne, and P. Joly, "Modeling and simulation of a grand piano," *Journal of the Acoustical Society of America*, vol. 134, no. 1, pp. 648–665, 2013.

[9] M. van Walstijn and J. Bridges, "Simulation of distributed contact in string instruments: a modal expansion approach," in *Proc. Europ. Sig. Proc. Conf. (EUSIPCO2016)*, 2016.

[10] S. Bilbao, *Numerical Sound Synthesis*. Chichester, UK: Wiley & Sons, 2009.

[11] V. Arnold, *Mathematical methods of classical mechanics*. New York: Springer, 1978, vol. 60.

[12] D. Greenspan, "Conservative numerical methods for $\ddot{x} = f(x)$," *Journal of Computational Physics*, vol. 56, no. 1, pp. 28–41, 1984.

[13] C. Issanchou, S. Bilbao, J. Le Carrou, C. Touzé, and O. Doaré, "A modal-based approach to the nonlinear vibration of strings against a unilateral obstacle: Simulations and experiments in the pointwise case," *Journal of Sound and Vibration*, vol. 393, pp. 229–251, 2017.